

AD-A203 735

DTIC FULL COPY

(1)

CMS Technical Summary Report #89-13

INSTABILITIES IN SHEAR FLOW OF  
VISCOELASTIC FLUIDS WITH  
FADING MEMORY

Bradley J. Plohr

UNIVERSITY  
OF WISCONSIN



CENTER FOR THE  
MATHEMATICAL  
SCIENCES

Center for the Mathematical Sciences  
University of Wisconsin—Madison  
610 Walnut Street  
Madison, Wisconsin 53705

September 1988

DTIC  
SELECTED  
FEB 08 1989  
S D  
D C 8

(Received September 28, 1988)

Approved for public release  
Distribution unlimited

Sponsored by

U. S. Army Research Office  
P. O. Box 12211  
Research Triangle Park  
North Carolina 27709

National Science Foundation  
Washington, DC 20550

89 2 6 144

UNIVERSITY OF WISCONSIN - MADISON  
CENTER FOR THE MATHEMATICAL SCIENCES

INSTABILITIES IN SHEAR FLOW IN VISCOELASTIC FLUIDS  
WITH FADING MEMORY

Bradley J. Plohr\*

CMS Technical Summary Report #89-13

September 1988



Account No.	100-100000000000
NTIS GEN. ED.	✓
DTIC Tel.	1
University of Wisconsin	1
Just for me	1
By _____	
Distribution:	
Approved by _____	
Dist	Agency _____ Special
A-1	

AMS (MOS) Subject Classifications: 35L60, 35L65, 35L67, 35L80, 35R05, 65M99,  
73F15, 73H99, 76A10.

Key Words: viscoelastic materials, fading memory, shear flow, spurt phenomenon, nonlinear conservation laws, mixed type, Riemann problems, random choice method.

---

\*Computer Science Department and Center for the Mathematical Science,  
University of Wisconsin-Madison, Madison, WI 53706.

---

Supported by the U. S. Army Research Office under Grant No. DAAL03-87-K-0036  
and by the National Science Foundation under Grant No. DMS-8712058.

# INSTABILITIES IN SHEAR FLOW OF VISCOELASTIC FLUIDS WITH FADING MEMORY \*

Bradley J. Plohr

Computer Sciences Department

and

Center for the Mathematical Sciences

University of Wisconsin-Madison

Madison, WI 53706

## 1. Introduction

For certain models of viscoelastic fluids with fading memory, classical steady channel flow does not exist beyond a maximal wall shear stress. This occurs when the shear stress for steady flow decreases with strain. For generalized Newtonian models of viscoelastic flow, such a decrease implies that the flow is unstable. Because of this example, a constitutive relation that exhibits a maximal wall shear stress is regarded as defective.

We report on work showing that, contrary to this intuition, such models correctly describe the experimentally observed "spurt" phenomenon: exceeding this critical stress results in a large increase in volumetric flow rate. The transition to spurt flow is analogous to a dynamically generated phase transition.

To analyze this phenomenon, we derive a system of conservation laws that govern the flow; these equations take the form of gas dynamics with relaxation terms. We solve the Riemann problem for this non-strictly-hyperbolic system, and incorporate this solution into the random choice method. Numerical simulation of channel flow, with the maximal wall shear stress exceeded, shows that a discontinuity forms at the wall, allowing the fluid to "slip"; no steady state exists. However, when a small Newtonian viscosity is included in the model, a "slip layer" forms and the flow approaches a discontinuous steady state.

## 2. Viscoelastic Fluids with Fading Memory

The motion of a fluid is defined by the spatial position  $\vec{x}(\vec{X}, t)$  at time  $t$  of each fluid particle  $\vec{X}$ . The velocity of a particle is then  $\vec{v} = \partial \vec{x} / \partial t$ . The deformation of the fluid is characterized by the deformation gradient  $F = \partial \vec{x} / \partial \vec{X}$ . Alternatively, the deformation undergone by the fluid from time  $s$  to time  $t$  may be specified using the relative deformation gradient  $F_s(t) = F(t)F(s)^{-1} = \partial \vec{x}(t) / \partial \vec{x}(s)$ . We will work in the Eulerian picture, so all fluid variables are regarded as functions of the spatial position  $\vec{x}$  at time  $t$ .

When the flow is incompressible and isothermal, the equations governing the evolution of  $F$  and  $\vec{v}$  are the continuity equation,

$$\dot{F} = (\nabla \vec{v})F , \quad (2.1)$$

and the conservation of momentum,

$$\rho \dot{\vec{v}} = \nabla \cdot \sigma . \quad (2.2)$$

Here  $\rho$  is the mass density,  $\sigma$  is the Cauchy stress, and a dot denotes the convective time derivative; also, the components of  $\nabla \vec{v}$  are  $(\nabla \vec{v})^i_j = \partial v^i / \partial x^j$ . We will write  $\sigma = -pI + \Sigma$ , where  $p$  is an isotropic pressure that maintains incompressibility;  $\Sigma$  is the extra stress.

The response characteristics of the fluid are embodied in the constitutive relation for the stress. For viscoelastic fluids with fading memory, these relations specify the extra stress as a functional of the deformation history of the fluid. Many sophisticated constitutive models have been devised; see Ref. [1] for a survey.

In the present work we focus on the Johnson-Segelman model [5] as a prototype for general constitutive models. This model accounts for non-affine deformation of Gaussian networks by introducing a parameter  $a$ ,  $-1 \leq a \leq 1$ , that enters a nonlinear generalization of the classical Maxwell model:

$$\Sigma = \int_{-\infty}^t m(t-s) \{ \bar{F}_s(t) \bar{F}_s(t)^T - I \} ds , \quad (2.3)$$

where  $\bar{F}_s$  satisfies

$$\dot{\bar{F}}_s = -R_a^T \bar{F}_s, \quad \bar{F}_s(s) = I. \quad (2.4)$$

Here  $R_a = \omega - ad$ , with  $d = \frac{1}{2} [\nabla \vec{v} + (\nabla \vec{v})^T]$  and  $\omega = \frac{1}{2} [\nabla \vec{v} - (\nabla \vec{v})^T]$  being the deformation rate and vorticity tensors. When  $a = 1$ ,  $\bar{F}_s = F_s$  and the Johnson-Segalman model reduces to the Maxwell model.

The function  $m$  is a memory kernel, defined on  $[0, \infty)$ , that we assume to be smooth, nonnegative, and integrable. A typical example is

$$m(s) = \mu \lambda e^{-\lambda s}, \quad (2.5)$$

where  $\mu$  is a shear modulus and  $\lambda$  is a relaxation rate. With this choice of memory kernel, the Johnson-Segalman model may be formulated as the differential equation

$$\dot{\Sigma} + \Sigma R_a + R_a^T \Sigma = 2a\mu d - \lambda \Sigma \quad (2.6)$$

for the extra stress.

Constitutive relations such as Eq. 2.6 exhibit a mixture of elastic and viscous behavior. This may be seen heuristically as follows. In the short relaxation-time limit,  $\lambda \rightarrow 0$ , Eq. 2.6 shows that an objective time derivative of  $\Sigma$  is proportional to the deformation rate:  $\dot{\Sigma} \sim 2a\mu d$ . This is characteristic of elastic behavior, and leads to the interpretation of  $a\mu$  as a shear modulus. By contrast, when  $\lambda, \mu \rightarrow \infty$  with  $\mu/\lambda$  fixed,  $\Sigma \sim 2(a\mu/\lambda)d$ ; thus, the model displays viscous behavior with  $a\mu/\lambda$  being the Newtonian shear viscosity coefficient.

As shown in Ref. [5], the constitutive relation for the stress derives from the energy

$$\mathcal{E} = \frac{1}{2a\rho} \int_{-\infty}^t m(t-s) \text{Tr} \{ \bar{F}_s(t) \bar{F}_s(t)^T - I \} ds. \quad (2.7)$$

The energy satisfies the conservation principle

$$\rho \left( \frac{1}{2} \vec{v} \cdot \vec{v} + \mathcal{E} \right) \cdot = \nabla \cdot (\vec{v} \cdot \sigma) - \rho r, \quad (2.8)$$

where

$$r = -\frac{1}{2a\rho} \int_{-\infty}^t m'(t-s) \operatorname{Tr} \{ \bar{F}_s(t) \bar{F}_s(t)^T - I \} ds \quad (2.9)$$

represents the rate of dissipation of energy.

### 3. Shear Flow

Interesting properties of viscoelastic constitutive relations are exhibited in simple planar shear flow. With the flow aligned along the  $y$ -axis, the deformation gradient  $F$  takes the form

$$F = \begin{pmatrix} 1 & 0 \\ \epsilon & 1 \end{pmatrix}, \quad (3.1)$$

where the strain  $\epsilon$  depends only on the spatial coordinate  $x$  and the time  $t$ . In particular, the flow is incompressible; we assume  $\rho$  to be constant throughout the fluid. Let  $v$  denote the  $y$ -component of  $\vec{v}$  and let  $\sigma$  denote the shear stress  $\Sigma^{xy} = \Sigma^{yx}$ . The variables  $v$ ,  $\sigma$ ,  $\Sigma^{xx}$ , and  $\Sigma^{yy}$  also depend only on  $x$  and  $t$ , while the pressure  $p$  takes the form  $p(x, y, t) = p_0(x, t) - f(t)y$ . The quantity  $f$  corresponds to a pressure gradient driving the flow.

In this notation, the continuity equation, Eq. 2.1, reduces to

$$\epsilon_t - v_x = 0, \quad (3.2)$$

and the  $y$ -component of conservation of momentum, Eq. 2.2, becomes

$$\rho v_t - \sigma_x = f. \quad (3.3)$$

Furthermore, the  $x$ -component of the conservation of momentum equation determines  $p_0$  through the equation  $p_x = (\Sigma^{xx})_x$ .

The stress components are expressed in terms of the history of the strain through the constitutive relation, Eq. 2.3. As is easily determined,

$$\sigma = \frac{a}{\alpha} \int_{-\infty}^t m(t-s) \sin(\alpha[\epsilon(t) - \epsilon(s)]) ds, \quad (3.4)$$

where  $\alpha = \sqrt{1 - a^2}$ . Similarly,  $\Sigma^{xx} = -\frac{1}{2}(1 - a)\mathcal{N}_1$  and  $\Sigma^{yy} = \frac{1}{2}(1 + a)\mathcal{N}_1$ , where  $\mathcal{N}_1 = \Sigma^{yy} - \Sigma^{xx}$  is the principal normal stress difference:

$$\mathcal{N}_1 = \frac{2a}{\alpha^2} \int_{-\infty}^t m(t-s) \{1 - \cos(\alpha[\epsilon(t) - \epsilon(s)])\} ds . \quad (3.5)$$

Also, the energy is given by  $\rho\mathcal{E} = \frac{1}{2}\mathcal{N}_1$ . Notice that  $\mathcal{N}_1 \geq 0$ .

In the special case when  $m$  is given by Eq. 2.5, Eqs. 3.2–5 imply the differential equations

$$\rho v_t - \sigma_x = f , \quad (3.6)$$

$$\sigma_t - [a\mu - \alpha^2 \rho\mathcal{E}] v_x = -\lambda\sigma , \quad (3.7)$$

$$\rho\mathcal{E}_t - \sigma v_x = -\lambda\rho\mathcal{E} . \quad (3.8)$$

Several mathematical results are known for this quasilinear system; see Ref. [10] for discussion and references.

- The system is strictly hyperbolic if and only if

$$\rho\mathcal{E} < \frac{a\mu}{\alpha^2} , \quad (3.9)$$

and the change of type has been associated to certain instabilities.

- For smooth, hyperbolic initial data with sufficiently small variation, a classical solution exists for all time.
- Nevertheless, smooth initial data exist for which the solution develops singularities within a finite time. As the critical time is approached, the spatial derivatives of  $v$  and  $\sigma$  become unbounded.

Thus, the fading memory acts as a weak dissipative mechanism: the source terms in the equations serve to counteract the formation of singularities from sufficiently smooth data. When singularities do form, however, Eqs. 3.6–8 are no longer valid because the products of distributions  $\mathcal{E}v_x$  and  $\sigma v_x$  are ill-defined. Instead, the physical conservation equations, interpreted in the sense of distributions, govern the flow.

#### 4. Equivalent Conservation Form

Eqs. 3.2–3 and 3.4 express physical conservation principles that remain valid past “blow-up.” They are not standard conservation laws, however, because the stress is given by a convolution integral. To solve these equations, we first derive an equivalent system of equations that is more amenable to analysis.

This system is obtained by introducing  $z \geq 0$  and  $\theta$  through the equations

$$z \cos(\alpha\theta) = m * \cos(\alpha\epsilon) , \quad (4.1)$$

$$z \sin(\alpha\theta) = m * \sin(\alpha\epsilon) , \quad (4.2)$$

where we use the convolution notation

$$m * \phi(\epsilon) = \int_{-\infty}^t m(t-s)\phi(\epsilon(s))ds . \quad (4.3)$$

Notice that  $z$  and  $\theta$  are continuous in  $t$  for almost every  $x$ , assuming that  $\epsilon$  is of bounded variation. Therefore, in calculating the distributional time derivatives of  $z$  and  $\theta$ , we may legitimately multiply by functions of  $z$  and  $\theta$ . Simple algebra shows that

$$z_t = m(0) \cos(\alpha[\epsilon - \theta]) + \cos(\alpha\theta) m' * \cos(\alpha\epsilon) + \sin(\alpha\theta) m' * \sin(\alpha\epsilon) , \quad (4.4)$$

$$\alpha z \theta_t = m(0) \sin(\alpha[\epsilon - \theta]) - \sin(\alpha\theta) m' * \cos(\alpha\epsilon) + \cos(\alpha\theta) m' * \sin(\alpha\epsilon) . \quad (4.5)$$

Furthermore, the stress components are given as functions of  $\epsilon$ ,  $z$ , and  $\theta$ :

$$\sigma = a\alpha^{-1} z \sin(\alpha[\epsilon - \theta]) , \quad (4.6)$$

$$\mathcal{N}_1 = 2a\alpha^{-2} \{\mu_{\text{tot}} - z \cos(\alpha[\epsilon - \theta])\} , \quad (4.7)$$

with  $\mu_{\text{tot}} = \int_0^\infty m(s)ds$ .

In this way, the constitutive relation 3.4 is transformed into Eq. 4.6 together with the conservation laws 4.4–5. The convolution integral that appeared in the definition of  $\sigma$  has been removed; in its place is a pair of evolution equations for the “internal variables”  $z$  and  $\theta$ . Because the stress depends on  $\epsilon$  and  $\theta$  only through the combination  $\tau = \epsilon - \theta$ ,  $\theta$  may be regarded as the unrecoverable, or “viscoplastic,” part of the strain, while  $\tau$  is the “elastic” strain.

## 5. Nonlinear Waves

Let us now restrict to the case of a single relaxation mode:  $m(s) = \mu \lambda \exp(-\lambda s)$ . If we eliminate  $\theta$  in favor of  $\tau = \epsilon - \theta$  by combining Eq. 4.5 with Eq. 3.2, then Eq. 3.2 for  $\epsilon$  decouples from the system. Therefore, we obtain the conservation laws

$$\tau_t - v_x = -\mu \lambda \alpha^{-1} z^{-1} \sin(\alpha \tau), \quad (5.1)$$

$$\rho v_t - \sigma(\tau, z)_x = f, \quad (5.2)$$

$$z_t = -\lambda \{z - \mu \cos(\alpha \tau)\} \quad (5.3)$$

together with the constitutive relation

$$\sigma(\tau, z) = a \alpha^{-1} z \sin(\alpha \tau). \quad (5.4)$$

In the present isothermal approximation, energy is not conserved in discontinuous flows. Rather, the energy equation, Eq. 2.8, serves as an “entropy” condition for weak solutions:

$$\rho \left[ \frac{1}{2} v^2 + \mathcal{E}(\tau, z) \right]_t - [\sigma(\tau, z)v]_x \leq vf - \lambda \rho \mathcal{E}(\tau, z) \quad (5.5)$$

where

$$\rho \mathcal{E}(\tau, z) = a \alpha^{-2} \{\mu - z \cos(\alpha \tau)\}. \quad (5.6)$$

Except for the presence of source terms, Eqs. 5.1–3 are identical to those for Lagrangian, homentropic gas dynamics, with  $\tau/\rho$  identified as specific volume,  $-\sigma$  as pressure, and  $z$  as a function of the entropy. Corresponding to the fundamental thermodynamic identity is

$$\rho d\mathcal{E} = \sigma d\tau + \rho T dz, \quad (5.7)$$

where  $T = -\rho^{-1} a \alpha^{-2} \cos(\alpha \tau)$  plays the role of “temperature.”

However, the equation of state, Eq. 5.6 or Eq. 5.4, would be rather peculiar for a gas; cf. Ref. [8]. The physical state of the fluid is unchanged if  $\tau$  is replaced by  $\tau + 2\pi/\alpha$ , so state space is cylindrical; for convenience, we require that  $-\pi/2 \leq \alpha \tau < 3\pi/2$ , along with

$z \geq 0$ . The wave speeds are  $\pm c$  and 0, where  $\rho c^2 = \partial\sigma/\partial\tau = az \cos(\alpha\tau)$  defines the sound speed  $c$ . Therefore the system is strictly-hyperbolic if  $-\pi/2 < \alpha\tau < \pi/2$ , whereas there is a complex-conjugate pair of purely imaginary wave speeds when  $\pi/2 < \alpha\tau < 3\pi/2$ . The wave mode with zero speed is linearly degenerate, and the sound modes with speed  $\pm c$  are genuinely nonlinear in the hyperbolic region except at  $\tau = 0$ .

Despite the peculiarities of the system, we have determined completely the structure of scale-invariant nonlinear waves. Such a wave consists of a sequence of elementary scale-invariant waves, either centered discontinuities or rarefaction waves, connecting constant states on the left and right. Discontinuities are required to satisfy Liu's generalization of Olešnik's entropy condition, which guarantees that the energy dissipation inequality 5.5 holds. This admissibility condition is equivalent to requiring shock waves to have viscous profiles: with Eq. 5.2 augmented by the Newtonian viscosity term  $(\eta v_x)_x$ , admissible shock waves arise as limits as  $\eta \rightarrow 0$  of travelling wave solutions.

The wave structure is conveniently depicted with a wave curve, the locus of states  $U = (\tau, v, z)$  on the right for a fixed state  $U_L = (\tau_L, v_L, z_L)$  on the left. Only  $z$  may change across waves with zero speed, so these wave curves are trivial. On the other hand,  $z$  remains constant across waves corresponding to the characteristic families with speeds  $\pm c$ , so we suppress the  $z$  component of  $U$  when drawing wave curves. Fig. 1 shows the wave curve of the  $-c$  family for a representative initial state  $U_L$ ; the wave curve of the opposite family is obtained by reflection through the vertical line  $v = v_L$ . The figure was produced using a computer program that constructs the wave curves for general systems of conservation laws [4]. Of particular interest is the manner in which the wave curve corresponding to the  $-c$  characteristic family continues past the boundary of the elliptic region with waves that contain rarefaction and shock waves of the  $+c$  family; this is possible because the wave speeds coincide at the elliptic region.

With the wave curves known, Riemann initial-value problems may be solved. We have written a computer program that solves Riemann problems, and have incorporated it into

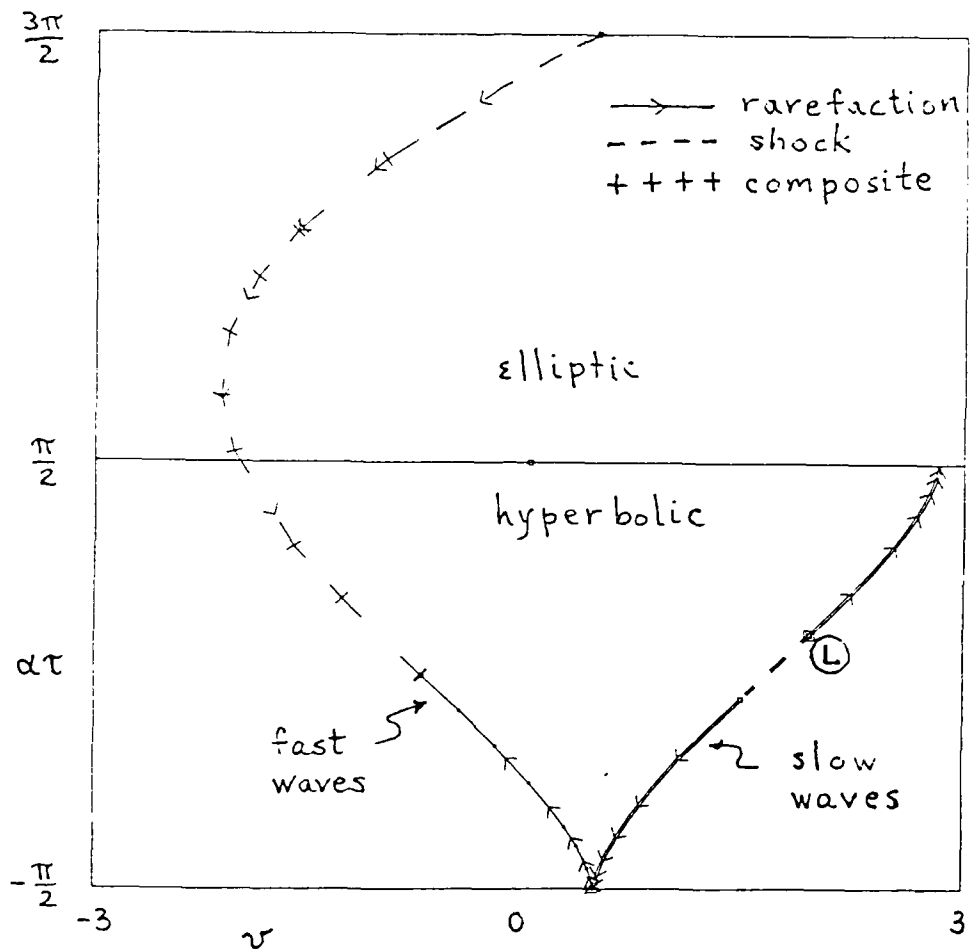


Fig. 1: The wave curve for a typical  $U_L$ . Solid curves correspond to rarefaction waves, dashed curves to shock waves, and dashed curves with crossbars to composite waves. Doubled curves represent the  $-c$  family, while single curves represent the  $+c$  family.

the Glimm-Chorin random choice method. We refer to Ref. [9] for a detailed discussion of this method. The Riemann problem solver can also be used in enhanced computational methods for two-dimensional flow problems, such as the front tracking method [2].

## 6. Steady Channel Flow

As an application of the results just described, we have investigated a flow of a Johnson-Segalman viscoelastic fluid in a channel [7]. In particular, we have studied the approach to steady flow, since this corresponds to rheological experiments.

Let the vertical walls of the channel be located at  $x = \pm \frac{1}{2}w$ . The flow is symmetric about the centerline ( $x = 0$ ), so we focus on the left half of the channel,  $-\frac{1}{2}w \leq x \leq 0$ . Symmetry requires that  $v_x = 0$  at the centerline, and the no-slip boundary condition imposes that  $v = 0$  at the wall.

Steady shear flow occurs when the velocity  $v$  is independent of time. In this case, the strain rate  $\kappa = \epsilon_t = v_x$  is constant in time, so that the stress  $\sigma$  coincides with

$$\sigma_{\text{steady}}(\kappa) = \frac{a}{\alpha} \int_0^\infty m(s) \sin(\alpha\kappa s) ds . \quad (6.1)$$

The steady solution may be determined by integrating, in turn, the ordinary differential equations  $-\sigma_{\text{steady}}(\kappa)_x = f$  and  $v_x = \kappa$ , with the boundary conditions that  $\kappa = 0$  at  $x = 0$  and  $v = 0$  at  $x = -\frac{1}{2}w$ .

Steady solutions may fail to exist if  $\sigma_{\text{steady}}(\kappa)$  does not vary monotonically with  $\kappa$ . For example, when  $m(s) = \mu\lambda \exp(-\lambda s)$ ,

$$\sigma_{\text{steady}}(\kappa) = \frac{a\mu}{\alpha} \frac{\alpha\kappa/\lambda}{1 + (\alpha\kappa/\lambda)^2} \quad (6.2)$$

attains a maximum  $\sigma_{\text{max}} = \frac{1}{2}a\mu/\alpha$  when  $\alpha\kappa/\lambda = 1$ . Classical steady flow in a channel of width  $w$  cannot exist if the pressure gradient  $f$  exceeds a critical value  $f_{\text{crit}}$  given by  $\sigma_{\text{max}} = \frac{1}{2}wf_{\text{crit}}$ . Notice that this phenomenon is not associated with loss of hyperbolicity, since  $\rho\mathcal{E} = \frac{1}{2}a\mu/\alpha^2$  at the stress maximum, well within the bound 3.9.

Traditionally, the non-existence of classical steady solutions caused by a shear stress maximum is regarded as a defect of the constitutive law. This conclusion is based on intuition appropriate for generalized Newtonian models of viscoelastic fluids. Shear flow for such a fluid is governed by the single equation

$$\rho v_t - [\eta(v_x)v_x]_x = f , \quad (6.3)$$

corresponding to having a viscosity coefficient  $\eta$  that depends on strain-rate. In a flow regime where  $\eta(\kappa)\kappa$  decreases with strain-rate  $\kappa$ , however, Eq. 6.3 has the character of a backward heat equation, which suffers from the Hadamard instability. Therefore, for generalized Newtonian fluids,  $\eta(\kappa)\kappa$  must increase with  $\kappa$  in a physically stable steady solution.

The Johnson-Segalman model has the same steady solutions as does a generalized Newtonian fluid with  $\eta(\kappa)\kappa = \sigma_{\text{steady}}(\kappa)$ , so one might think that it exhibits the same instability in regions where  $\sigma_{\text{steady}}$  decreases. This conclusion is not warranted, however, because the system of equations maintains its evolutionary character even near the shear stress maximum.

A question remains: what is the solution if the critical pressure gradient  $f_{\text{crit}}$  is exceeded? To answer this we must solve the time-dependent equations, allowing for the possible formation of singularities.

## 7. Slip and Spurt Phenomena

We have simulated numerically a simple experiment for a fluid governed by the system 5.1–4. Without loss of generality, units are chosen so that  $a\mu = 1$ ,  $\lambda = 1$ , and  $\rho = 1$ , and the fluid variables are scaled so that  $a$  disappears from the equations. Given this choice, the channel thickness  $w$  and the pressure gradient  $f$  (which depends on time) are the essential parameters defining the flow. In the numerical experiment, the channel width is  $w = 1$ , so that the wall of the channel is located at  $x = -\frac{1}{2}$  while the center is at  $x = 0$ . The flow is initially in the classical steady state corresponding to the critical pressure gradient  $f_{\text{crit}}$ ; then the pressure gradient is increased abruptly to the super-critical value  $1.2f_{\text{crit}}$ .

The result of this calculation using the random choice method is shown in Fig. 2. The fluid velocity  $v$  is plotted vs. position  $x$  at successive time intervals; generally the velocity increases with time. During the early stages of the experiment, the flow settles into a

quasi-steady state. This effect is especially evident in a plot of the centerline velocity as a function of time, and it is more pronounced when the channel width  $w$  is smaller [7]. Eventually, however, a thin layer develops at the wall in which the velocity rises to a value that is nearly constant across the channel. For practical purposes, the fluid has broken free from the wall and is accelerating uniformly under the applied pressure gradient; thus the fluid "slips."

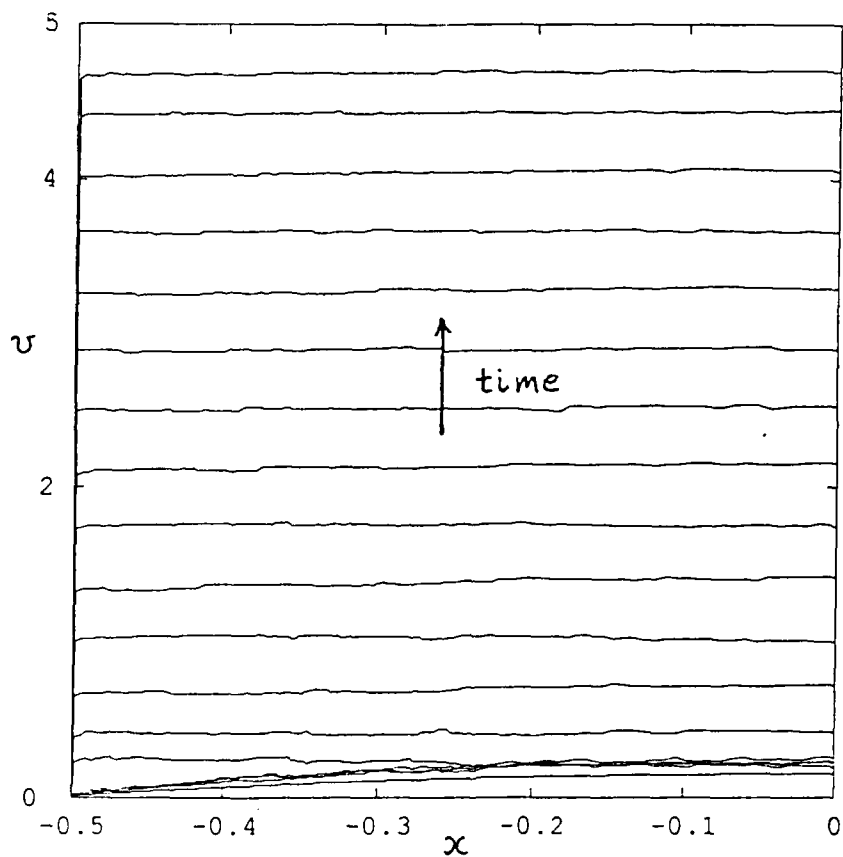


Fig. 2: Onset of slip for a fluid without Newtonian viscosity.

To understand this result better, the same experiment was performed for a fluid that has a small, but nonzero, Newtonian viscosity (e.g., because of the presence of a solvent). For such a fluid, the term  $(\eta v_x)_x$  is added to the right-hand-side of Eq. 5.2. So long as  $0 \leq \eta < 1/9$  (in dimensionless units), the steady shear stress, plotted vs. strain, still exhibits a maximum.

Fig. 3 shows the results for  $\eta = 0.01$ , as calculated using the Lax-Wendroff method with Tyler artificial viscosity. Now the slip layer is much thicker, with its outer boundary corresponding to a discontinuity in the strain rate  $v_x$ . The solution approaches a steady state in which  $v_x$  is discontinuous but the total stress  $\sigma_{\text{steady}}(v_x) + \eta v_x$  is continuous.

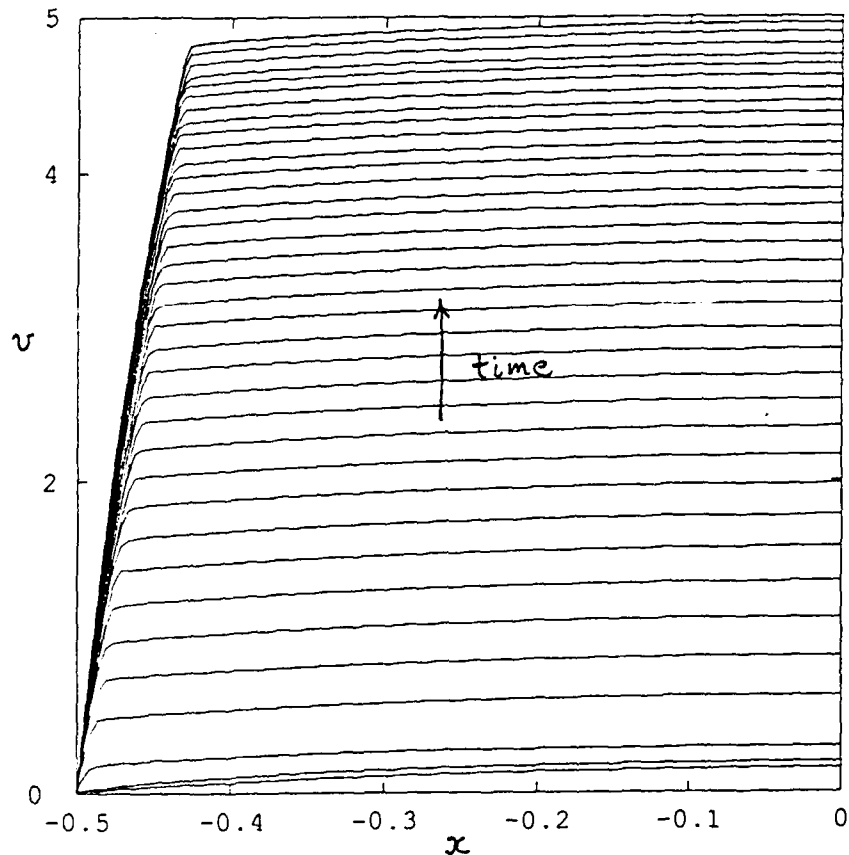


Fig. 3: Onset of spurt for a fluid with Newtonian viscosity.

Further study of channel flow for a Johnson-Segalman fluid yields several observations [7].

- The nominal shear rate (based on volumetric flow rate), plotted against the nominal shear stress (based on the pressure gradient), shows an abrupt increase at a critical point, i.e., "spurt."
- The thickness of the slip layer (or, equivalently, the stress at which the strain-rate discontinuity occurs) exhibits hysteresis as a function of the loading.

- There are three essential time scales to the flow problem, corresponding to processes governed by Newtonian viscosity, by wave propagation, and by relaxation. In some situations this leads to a quasi-steady supercritical flow that persists for a time orders of magnitude longer than the wave propagation scale.

There are two essential features responsible for spurt and hysteresis phenomena in viscoelastic models: (1) a non-monotone stress-strain relation in steady flow; and (2) a dynamical mechanism for selecting steady shock waves that are physical. For example, the spurt and hysteresis phenomena were analyzed by Hunter and Slemrod [3] for a related, but simpler, model of a viscoelastic fluid. Their analysis shows how the first two observations may be understood, and we expect that it may be applied to the present model. We emphasize, however, that the Johnson-Segalman model differs in an essential way from the model considered by Hunter and Slemrod: it remains hyperbolic even in the range where the stress decreases with strain, as is desirable for equations that describe evolution of a physical system.

Spurt and hysteresis offers an explanation of certain observations in rheological experiment [11]. Quantitative agreement between experiment [11] and Johnson-Segalman model has been verified in Ref. [6]. Therefore, we have confidence that the interesting mathematical structure of models of viscoelastic flow reflects observable physical phenomena.

### Acknowledgements

The author thanks Profs. D. Malkus and J. Nohel for introducing him to viscoelastic flows, and for many discussions that contributed to the present work. He also thanks Profs. M. Johnson and T-P. Liu for their encouragement and useful comments.

### References

1. R. Bird, R. Armstrong and O. Hassager, *Dynamics of Polymeric Liquids*, John Wiley and Sons, New York, 1987.

2. J. Glimm, C. Klingenber, O. McBryan, B. Plohr, D. Sharp and S. Yaniv, "Front Tracking and Two Dimensional Riemann Problems," *Adv. Appl. Math.* **6** (1985), pp. 259-290.
3. J. Hunter and M. Slemrod, *Phys. Fluids* **26** (1983), pp. 2345-2351.
4. E. Isaacson, D. Marchesin and B. Plohr, "Construction of Nonlinear Waves for Conservation Laws," in preparation, 1988.
5. M. Johnson and D. Segalman, "A Model for Viscoelastic Fluid Behavior which Allows Non-Affine Deformation," *J. Non-Newtonian Fluid Mech.* **2** (1977), pp. 255-270.
6. R. Kolkka, D. Malkus, M. Hansen, G. Ierley and R. Worthing, "Spurt Phenomena of the Johnson-Segalman Fluid and Related Models," Preprint, Michigan Technical University, Houghton, MI, 1987.
7. D. Malkus, J. Nohel and B. Plohr, "Spurt and Slip Phenomena in Shear Flows of Non-Newtonian Fluids," in preparation, 1988.
8. R. Menikoff and B. Plohr, "The Riemann Problem for Fluid Flow of Real Materials," Preprint LA-UR-88-49, Los Alamos National Laboratory, Los Alamos, NM, 1988.
9. B. Plohr, "Shockless Acceleration of Thin Plates Modeled by a Tracked Random Choice Method," *AIAA J.*, 1988. To appear.
10. M. Renardy, W. Hrusa and J. Nohel, *Mathematical Problems in Viscoelasticity*, Pitman Monographs and Surveys in Pure and Applied Mathematics, Vol. 35, Longman Scientific & Technical, Essex, England, 1987.
11. G. Vinogradov, A. Malkin, Yu. Yanovskii, E. Borisenkova, B. Yarlykov and G. Berezhnaya, "Viscoelastic Properties and Flow of Narrow Distribution Polybutadienes and Polyisoprenes," *J. Polymer Sci., Part A-2* **10** (1972), pp. 1061-1084.